UNIVERSITY of York

This is a repository copy of *X-ray laser pulses at the Fourier transform limit*.

White Rose Research Online URL for this paper:
https://eprints.whiterose.ac.uk/id/eprint/2437/

Article:
Tallents, G.J. orcid.org/0000-0002-1409-105X, Edwards, M.H. and Mistry, P. (2007) X-ray laser pulses at the Fourier transform limit. Physical Review A. 013818. -. ISSN: 1094-1622

https://doi.org/10.1103/PhysRevA.75.013818

Reuse
Items deposited in White Rose Research Online are protected by copyright, with all rights reserved unless indicated otherwise. They may be downloaded and/or printed for private study, or other acts as permitted by national copyright laws. The publisher or other rights holders may allow further reproduction and re-use of the full text version. This is indicated by the licence information on the White Rose Research Online record for the item.

Takedown
If you consider content in White Rose Research Online to be in breach of UK law, please notify us by emailing eprints@whiterose.ac.uk including the URL of the record and the reason for the withdrawal request.

White Rose university consortium
Universities of Leeds, Sheffield & York

eprints@whiterose.ac.uk
https://eprints.whiterose.ac.uk/

promoting access to White Rose research papers

Universities of Leeds, Sheffield and York
http://eprints.whiterose.ac.uk/

This is an author produced version of a paper published in **Physical Review A**.

White Rose Research Online URL for this paper:
http://eprints.whiterose.ac.uk/2437/

Published paper
Mistry, P., Tallents, G.J. and Edwards, M.H. (2007) *X-ray laser pulses at the Fourier transform limit.* Physical Review A, 75 (1). Art. No. 013818.

White Rose Consortium ePrints Repository
eprints@whiterose.ac.uk

X-ray laser pulses at the Fourier transform limit.

P. Mistry, G.J. Tallents and M.H. Edwards.

Department of Physics, University of York, York, YO10 5DD, United Kingdom.

Abstract

The temporal output of a Ni-like Ag x-ray laser of wavelength 13.9 nm has been recorded using a streak camera with ultra-short (700 fs) temporal resolution. We present a model to calculate the degree of coherence and Fourier transform limit of x-ray laser pulses produced by amplified spontaneous emission and relate the results from the model to previous interferometric measurements of the coherence length of the same Ni-like Ag x-ray laser and our measured duration of temporal output. Our modeling shows that the interferometer and streak camera results are consistent and close to the Fourier transform limit at longer gain medium lengths.

I. Introduction

Saturated x-ray lasing at wavelengths in the range 5.9 – 30 nm [1, 2] and with pulse durations down to $\approx$ 3 ps [3, 4] has been produced in plasmas pumped by optical lasers. In these experiments, a first laser pulse incident onto a solid in a line focus creates a pre-formed plasma of Ne- or Ni-like ionization and a second pulse heats free electrons that produce population inversions by monopole electron collisional excitation. Lasing occurs in Ne- or Ni-like ions between 3p – 3s and 4d – 4p levels respectively as the upper levels are metastable to decay to the ground 2p and 3d states respectively [1, 2]. It has been shown that this mechanism of pumping x-ray lasers works with pumping laser pulses of duration from $\approx$100 ps down to < 1 ps, but that gain is always present for times $\geq$ 10 ps with minimum observed x-ray lasing duration of $\approx$3 ps [3].

Observations of x-ray lasing arise from amplified spontaneous emission (ASE) and mirrors are not needed. With plasma based x-ray lasers, the output is spectrally narrow ($\upsilon/\Delta\upsilon > 10^4$) due to gain narrowing of the already spectrally narrow Doppler or pressure broadened gain profile. Koch *et al*. [5] constructed a spectrometer with a spectral resolving power of 35000 and measured x-ray laser spectral widths. Similar direct measurements of the linewidth have been conducted by G. Yuan *et al* [6]. Other measurements of the spectral profiles of x-ray lasers have been undertaken using interferometry [7 – 9]. The longitudinal coherence length and hence the spectral output of the x-ray laser can be measured by recording fringe visibility as a function of the difference in optical path length of an interferometer [10].

From estimates of the frequency width of the gain coefficient of x-ray lasers, x-ray laser pulses of ≈ 3 ps duration are calculated to be close to the Fourier transform limit [3, 4, 8]. However, there has not been a direct measurement of the frequency bandwidth of x-ray laser output alongside a measurement of the pulse duration of the same x-ray laser pulses. There are, in addition, several features of the interpretation of frequency bandwidth from interferometric measurements and the determination of the exact Fourier transform relationships between frequency bandwidth and the pulse duration that have not previously been clarified for x-ray lasing produced by ASE.

The frequency bandwidth of the Laboratoire pour l'Utilisation des Lasers Intenses (LULI) x-ray laser operating with Ni-like Ag at 13.9 nm wavelength at Ecole Polytechnique in Paris has been measured using a Fresnel bimirror interferometer [9]. In this paper, we report measurements of the temporal duration of this x-ray laser using an ultra-fast streak camera. A model is introduced that relates the fringe visibility of interferometry results to the frequency bandwidth of the gain coefficient and evaluates the Fourier transform limit allowing for gain narrowing in ASE lasers. Using the model, the proximity of the LULI x-ray laser to the Fourier transform limit is demonstrated and analysed.

II. Experiment

X-ray lasing at 13.9 nm in a 4d – 4p Ni-like silver line has been produced with double pulse pumping at the LULI laser facility. The background pulse was 600 ps in duration with an intensity of 10^{12} Wcm^{-2} and was followed by a 400 fs duration pulse of peak intensity 10^{15} Wcm^{-2}. The two pulses were separated by a peak-to-peak time

of 250 ps and were focused to lines of widths of 200 μ m and 60 μ m respectively onto a silver slab target.

A scanning Fresnel bimirror wavefront division interferometer has been used to investigate the longitudinal coherence of the 13.9 nm Ni-like silver x-ray laser pumped by the LULI laser [9]. Interferometry results were recorded for a L = 10 cm target length with the Fresnel bimirror located 3.5 m from the x-ray laser target. By varying the optical path length difference between the two arms of the interferometer, the fringe visibility as a function of path length difference up to 1.4 mm was measured [9].

The temporal variation of the 13.9 nm Ni-like silver x-ray laser pumped by the LULI laser has been measured using a fast streak camera with a KI photocathode, 700 fs resolution and ~ 5 ps mm^{-1} sweep rate [11] for a range of target lengths. The streak camera has a limited dynamic range of the incident x-ray intensity arising from the rapid streak rate, but this has been characterised in previous experiments. Using filters care was always taken to operate the streak camera with sufficiently low incident x-ray laser intensities to avoid saturation effects on the pulse duration measurements. The x-ray laser output was relayed to the streak camera via a plane and spherical multilayer imaging mirror and a gold surface grazing-incidence reflection over a path of 6 m from the x-ray laser target. The multilayer mirror reflected over a narrow wavelength range (less than 1.5 nm). Together with 0.2 μ m thick zirconium filters, this ensured that only the x-ray laser output was recorded by the streak camera.

III. Theory

A. Effect of short duration pulses on fringe visibility

When interfering beams of equal intensity, the visibility of fringes is equal to the degree of coherence γ of the two beams. However, the absolute scaling of the visibility with γ recorded in an interferometer needs to be adjusted if there are mismatches in intensity between the interfering beams. For pulse durations much longer than the coherence time, the relationship between visibility and γ is a constant (< 1) with optical path difference. We show quantitatively here that using interferometry to measure fringe visibility for pulses close to the Fourier transform limit results in a reduction in visibility that increases with the optical delay [12].

Considering laser output of Gaussian temporal shape, the electric fields of the two interfering pulses in an interferometer can be written as.

$$E_{1,2}(t) = E_{1,2}\exp\left[-2\ln(2)\left(\frac{t}{T}\right)^2\right] \tag{1}$$

where T is the FWHM pulse duration of the light intensity. When $c\Delta t$ is the path difference present between the two arms of the interferometer for c the speed of light, the maximum $I_{\max} \propto \int \left|E_1(t) + E_2(t+\Delta t)\right|^2 dt$ and minimum

$I_{\min} \propto \int \left|E_1(t) - E_2(t+\Delta t)\right|^2 dt$ average intensities in an interferometer can be calculated. The fringe visibility is given by

$$V(\Delta t) = \frac{\int \left|E_1(t) + E_2(t+\Delta t)\right|^2 dt - \int \left|E_1(t) - E_2(t+\Delta t)\right|^2 dt}{\int \left|E_1(t) + E_2(t+\Delta t)\right|^2 dt + \int \left|E_1(t) - E_2(t+\Delta t)\right|^2 dt}. \tag{2}$$

For Gaussian temporal profiles (equation 1) this leads to [13]

$$V(\Delta t) = \frac{2E_1E_2 \exp\left[-\ln(2)\left(\frac{\Delta t}{T}\right)^2\right]}{E_1^2 + E_2^2}\gamma(\Delta t), \tag{3}$$

Equation 3 is identical to that developed by, for example, Born and Wolf [10] for the visibility in an interferometer except for the factor $f(\Delta t) = \exp\left[-\ln(2)\left(\frac{\Delta t}{T}\right)^2\right]$ allowing for the pulse duration T.

We can write generally for the visibility of fringes in an interferometer

$$V(\Delta t) = \frac{2E_1E_2}{E_1^2 + E_2^2} f(\Delta t)\gamma(\Delta t), \tag{4}$$

where the value of $f(\Delta t)$ is dependent on the shape of the pulse. Experimental work using fast streak cameras has found that the temporal profiles of x-ray laser pulses are closer to fitted asymmetric sech functions. The corresponding electric fields have the following form

$$E_{1,2}(t) = \frac{E_{1,2}}{\sqrt{\exp\left(\frac{At}{T}\right) + \exp\left(\frac{-Bt}{T}\right)}} \tag{5}$$

where A and B are constant values chosen to fit the experimental temporal profiles. The f value for the asymmetric sech function has been solved numerically. Figure 1

shows the behaviour of f with optical path difference for Gaussian and asymmetric sech pulse profiles with A=1 and B=8. All temporal pulse shapes give a decrease in f with optical path difference and hence have a greater effect for longer path differences.

B. The effect of gain narrowing on the degree of coherence

To be able to model the degree of coherence γ of the x-ray laser we need to calculate the spectral variation in the intensity. We can write for a normalized lineshape function $g(\nu)$ that $\phi(\nu) = g(\nu)/g(0)$ where frequency ν is measured from the line center. For Gaussian, Lorentzian and Voigt profiles respectively

$$\phi_G(\upsilon) = \exp\left(-4\ln 2\left(\frac{\upsilon}{\Delta\upsilon_G}\right)\right), \tag{6}$$

$$\phi_L(\upsilon) = \frac{1}{1+\left(\frac{2\upsilon}{\Delta\upsilon_L}\right)^2}, \tag{7}$$

and

$$\phi_v(\upsilon) = \frac{[\phi_G * \phi_L]_\nu}{[\phi_G * \phi_L]_{\nu=0}} \tag{8}$$

where $\Delta\upsilon_G$, $\Delta\upsilon_L$ are the full width at half maximum (FWHM) of the Gaussian and Lorentzian profiles respectively and $*$ is the convolution operation.

The degree of coherence $\gamma(\Delta t)$ and the spectral variation in a source of intensity $I(\nu)$ are related through a Fourier transform [10] such that

$$\gamma(\Delta t) = \frac{\int_{-\infty}^{\infty} I(\upsilon)\exp(-2\pi i \Delta t \upsilon) d\upsilon}{\int_{-\infty}^{\infty} I(\upsilon) d\upsilon} \tag{9}$$

where $\Delta d = c\Delta t$ is the optical path difference in one arm of an interferometer. For an x-ray laser, the source intensity profile $I(\upsilon)$ can be expressed as

$$I(\upsilon) = I_0 g(0)[\exp(G(0)L\phi(\upsilon)) - 1] \tag{10}$$

where $G(0)L$ is the actual gain coefficient length product at line center and $g(0)$ is the normalized lineshape function for the gain coefficient at line center. The x-ray laser theory derived by Pert [14] and Casperson [15] gives an approximation for the saturation effects on the spontaneous and stimulated emission for a homogenous laser expressed as

$$g_0 L = \frac{2I_0}{I_s}\alpha(G(0)L) + \left[1 - \frac{2I_0}{I_s}\right] G(0)L \tag{11}$$

where g_0 is the small signal gain coefficient at line centre, $\alpha(G(0)L)$ is an amplification factor which is a function of the actual gain coefficient length product $G(0)L$, I_0 is a measure of the spontaneous emission at line centre and I_s is the saturation intensity. We assume homogeneous broadening in this paper as Pert [14] has shown that gain coefficient profiles are homogenised due to minor collisional broadening components. This leads to the situation assumed for the later analysis of experimental results where the gain coefficient is homogeneous and Gaussian shaped with a width largely determined by thermal Doppler broadening. We also consider

Lorentzian and Voigt gain coefficient profiles in this theory section and show that results for the degree of coherence and Fourier transform limit are similar to those for Gaussian shaped gain coefficient profiles, particularly at longer gain length products.

Equations 9 and 10 allow us to express the degree of coherence as

$$\gamma(\Delta t) = \int_0^\infty [\exp(G(0)L\phi(\upsilon)) - 1]\exp(-i2\pi\Delta t\upsilon)d\upsilon\,. \qquad (12)$$

Figure 2 shows the spectral profiles for a Gaussian gain coefficient profile calculated using equations 6 and 10 assuming homogeneous broadening. The spectral width decreases with increasing actual gain coefficient length product *G(0)L* due to gain narrowing. Using equations 6 and 12 we can calculate the subsequent degree of coherence for different gain length products (figure 3). The Fourier transform of the gain narrowed spectral profiles gives an increasing width with increasing *G(0)L* for the degree of coherence profiles. The spectral intensity variation for a Lorentzian gain profile has been calculated in a similar way using equations 7 and 10 (figure 4). We find that the intensity profile remains Lorentzian for low *G(0)L*, but at the higher *G(0)L* values the profiles become Gaussian-like in shape. The degree of coherence for a Lorentzian gain profile is shown in figure 5. A Lorentzian function Fourier transforms to an exponential decay function of the form $\exp(-|t\Delta\upsilon_L|)$. We see that at low *G(0)L* the degree of coherence follows an exponential decay profile, while at larger *G(0)L* values the variation of the degree of coherence approaches a Gaussian shape.

We have calculated the spectral profile and the resultant degree of coherence for a sample Voigt profile of the gain coefficient (figures 6 and 7) calculated from equations 6 – 8, 10 and 12. The Voigt profile is produced by convoluting a Gaussian profile with a Lorentzian profile of equal spectral width. We find that the spectral gain narrowing behaviour and the subsequent change in the degree of coherence profile is similar to the Lorentzian profile.

We can define the coherence length of a source as the FWHM in optical path length difference $\Delta t \Delta \upsilon$ of the degree of coherence $\gamma(\Delta t)$ [16]. Here $\Delta \upsilon$ is the frequency bandwidth (FWHM) of the gain coefficient. From figures 3, 5 and 7 we can plot the variation in coherence length with actual gain coefficient length product *G(0)L* (figure 8). There is little difference in the results for Gaussian, Voigt and Lorentzian profiles, but there is a small variation with the value of the gain length product *G(0)L*.

IV. Comparison to experiments

A. The LULI x-ray laser

Figure 9 shows the variation of fringe visibility as a function of optical path length difference measured by Klisnick *et al*. [9] together with adjusted visibilities as outlined in section IIIA to allow for the short duration of the output pulses measured with a streak camera. Superimposed on figure 9 are values of the degree of coherence calculated as outlined in section IIIB for a Gaussian gain coefficient of bandwidth 6.5×10^{11} Hz for different gain length *G(0)L* values. The calculated degree of coherence values are adjusted in amplitude by a multiplying factor of 0.41 for all optical path length differences to fit the visibility data. This is justified as various effects can uniformly reduce the visibility. For example, the interfering beams can be

of unequal intensity or transverse coherence effects can be important. In our analysis, we assume that there are no changes in transverse coherence with changes in the longitudinal optical path length.

The fit of our theory to the Klisnick *et al*. [9] experimental data of figure 9 is worse than for previous x-ray laser coherence measurements [7, 8] (discussed later, see our figures 12 – 14). There are large shot – to – shot variations in the figure 9 visibilities possibly arising because of random changes in transverse coherence. For example, there is a range from 0.31 – 0.46 at zero path difference. Nevertheless, a gain-length product $G(0)L \approx 18$ and gain coefficient frequency bandwidth $\Delta\nu = 6.5 - 9.5 \times 10^{11}$ Hz approximately fits the experimental fringe visibilities of figure 9 (only $\Delta\nu = 6.5 \times 10^{11}$ Hz is shown on figure 9, see figure 3 for the effect of increasing $\Delta\nu$). A gain coefficient $G(0) \approx 18\,\mathrm{cm}^{-1}$ for the L = 1 cm medium is consistent with a measurement of the gain coefficient from a scan of X-ray laser flux as a function of length obtained using our streak camera and with previous experiments for this x-ray laser [17]. A gain coefficient $G(0) \approx 18\,\mathrm{cm}^{-1}$ indicates operation well into saturation for lengths $L \geq$ 5 mm with a small signal gain coefficient $g_0 \approx 32\,\mathrm{cm}^{-1}$ obtained using equation 11 with the assumption that $I_0/I_s = 10^{-6}$. Simulations with the EHYBRID fluid code with a RAYTRACE post-processor [18] predict an almost identical small signal gain coefficient of $g_0 = 30\,\mathrm{cm}^{-1}$. EHYBRID calculates the gain coefficient and electron density profiles normal to the target surface by solving the fluid equations coupled to atomic physics calculations of quantum state populations. The RAYTRACE post-processor uses the EHYBRID gain and electron density profiles to calculate X-ray

laser output assuming amplified spontaneous emission along ray paths subject to refraction.

New results showing the variation of the output pulse duration as a function of target length measured using the fast streak camera on the LULI x-ray laser are presented in figure 10. The pulse duration is predicted to drop with increasing target length L according to the EHYBRID/RAYTRACE [18] simulation (also shown on figure 10) rather than increase as observed experimentally. Diffraction and other wave properties of the laser light are not considered in these simulations. Wave effects on the pulse shape $I(t)$ due to the transform limit can be found from the Fourier transform of the electric field variation in frequency $E(\upsilon)$ (from equation 10) giving $E(t)$. The intensity is then calculated using $I(t) = \frac{1}{2}\varepsilon_0 c[E(t)]^2$. The Fourier transform limited pulse durations found using this procedure are dependent upon the gain bandwidth $\Delta\upsilon$ and the gain-length product $G(0)L$ and increase with target length L in agreement with the experimental observations. Using the values found from the fits to the longitudinal visibility data of figure 9, figure 10 includes some sample temporal durations for the expected Fourier transform limit. The Fourier transform values for $\Delta\nu = 6.5 \times 10^{11}$ Hz and $G(0) \approx 18\,\mathrm{cm}^{-1}$ when convoluted with the EHYBRID/RAYTRACE prediction give values approaching the experimental pulse duration variation.

The numerical RAYTRACE temporal profiles and the Fourier transform of the appropriate electric field variations arising from equation 10 can be convoluted together and superimposed on experimentally measured temporal profiles of x-ray

laser output. A worst case example is shown in figure 11 assuming $\Delta\nu = 9.5 \times 10^{11}$ Hz (the upper bound for the frequency bandwidth for the experimental data of figure 9). The agreement between the experimentally measured x-ray laser pulse variations and the RAYTRACE simulation convoluted with the Fourier transform temporal 'smearing' effect is good. This procedure and the results of figure 10 show that the dominant effect contributing to the X-ray laser pulse duration for longer lengths of x-ray laser medium arises from the Fourier transform limit.

The frequency bandwidth for the gain coefficient of $\Delta\nu = 6.5 - 9.5 \times 10^{11}$ Hz obtained from the published visibility plot (figure 9) implies ion temperatures of 17 - 35 eV assuming Doppler broadening of the gain coefficient. However, EHYBRID simulations predict that ion temperatures of 70 eV are present in the peak gain region of the plasma. Dicke narrowing of the Doppler line profile due to ion-ion collisions could explain this discrepancy [19]. From EHYBRID simulations, we estimate that the ratio Γ of ionic electrical potential energy and ionic thermal energy is such that $\Gamma \approx 0.3$ in the gain region of the plasma. The calculations of Griem [20] suggest that Dicke narrowing may occur for these Γ values, though molecular dynamic simulations of Pollack and London [21] indicate that Dicke narrowing only becomes important for $\Gamma > 5$. The discrepancy in ion temperature between the experimental bandwidth measurement and simulation has been discussed by Guilbaud et al [22] who suggest that random changes in transverse coherence with a limited number of observations have affected the interferometric measurements and hence would cause the bandwidth to be underestimated in our analysis. However, this argument is not consistent with the agreement of the streak camera results (e.g. figure 11) with our calculated temporal variations in laser output (taking account of ray tracing

simulations convoluted with transform limit effects using the interferometrically measured $\Delta\nu$).

B. Other x-ray lasers

Our Fourier transform limit modeling has been fitted in a similar manner as described above to longitudinal coherence measurements by Celliers *et al.* [7] and Smith *et al.* [8] (see figures 12 – 14). The Celliers *et al*. experiment used a single long pulse (600 ps) laser pump and so the gain coefficient was low at $G(0) \approx 5.3 \pm 0.5\,\mathrm{cm}^{-1}$ [23]. A Gaussian with 1/e half-half-width of 100 μm was fitted to the experimental visibility variation with optical path length by the authors. Our calculated visibility plots assuming Gaussian gain coefficient profiles have been fitted to this experimental visibility assuming $G(0)L = 7$ (see figure 12). In addition, the variation of visibility for a Gaussian shaped intensity profile for the x-ray laser is also superimposed on figure 12. For the Celliers *et al.* results, the fitting of our calculated γ to the published visibility results gives $\Delta\upsilon_G = 4.0\times10^{12}$ Hz and so implies an ion temperature of 780 eV assuming that the gain coefficient is Doppler broadened. Simulations by Celliers *et al.* predicted ion temperatures of 600 eV in the gain region [7]. The ion temperature from the bandwidth quoted by Celliers *et al*. [7] was ~ 125 eV, clearly different to their fluid code simulation. The ion temperature deduced using our visibility calculation is much closer to the temperature predicted by the code.

Smith *et al*. [8] used a Michelson interferometer to measure the frequency bandwidth of a 14.68 nm Ni-like Pd x-ray laser. Fringe visibility measurements were taken for two different pumping beam durations of 6 and 13 ps. The resulting visibility plots

were fitted with Gaussians with 1/e half-half-widths of 342 and 400 μm respectively by Smith *et al*. The Smith *et al*. visibility data is now fitted with our calculated visibility plots assuming Gaussian gain coefficient profiles for $G(0)L = 18$ in figures 13 and 14. A value of $G(0)L = 18$ is consistent with the small signal gain coefficient of g_0=65 cm^{-1} simulated by Smith *et al*. [8] for the $L = 1.25$ cm medium length. Our fitting implies an ion temperature of 120 or 150 eV for figures 13 and 14 respectively assuming the gain coefficient is Doppler broadened.

V. Conclusion

We have developed a model to calculate the degree of coherence of an x-ray laser source and evaluate the Fourier transform limit of x-ray laser pulses produced by ASE. The model includes gain narrowing effects and the effect of pulse duration on measurements of longitudinal coherence for pulses close to the Fourier transform limit. Measurements of the temporal duration of a Ni-like Ag x-ray laser are presented and shown to be consistent with previous measurements of the longitudinal coherence. Our modeling shows that the temporal durations and longitudinal coherence are consistent and close to the Fourier transform limit at longer gain medium lengths.

Acknowledgements

We thank O. Guilbaud, D. Ros and A. Klisnick for access and help with the x-ray laser temporal measurements. We would like to thank Dr. M. Kalal, Dr. A. Klisnick and Professor G. J. Pert for discussions on the work. Funding from the European Union LASERLAB, the L.E.A (Laboratoire Européen Associé) and the U.K. Engineering and Physical Sciences Research Council is gratefully acknowledged.

References

[1] G. J. Tallents, J. Phys D: Appl. Phys. **36**, R 259 (2003).

[2] H. Daido, Rep. Prog. Phys. **65**, 1513-1576 (2002).

[3] Y. Abou-Ali, G. J. Tallents, M. Edwards, R. E. King, G. J. Pert, S. J. Pestehe, F. Strati, R. Keenan, C. L. S. Lewis, S. Topping, O. Guilbaud, A. Klisnick, D. Ros, R. Clarke, D. Neely, M. Notley and A. Demir, Opt. Comm. **215**, 397 (2003).

[4] A. Klisnick, J. Kuba, D. Ros, R. Smith, G. Jamelot, C. Chenais-Popovics, R. Keenan, S. J. Topping, C. L. S. Lewis, F. Strati, G. J. Tallents, D. Neely, R. Clarke, J. Collier, A. G. MacPhee, F. Bortolotto, P. V. Nickles, and K. A. Janulewicz, Phys. Rev. A, **65**, 033810 (2002).

[5] J. A. Koch, B. J. MacGowan, L. B. Da Silva, D. L. Matthews, J. H. Underwood, P. J. Batson, and S. Mrowka, Phys. Rev. Lett., **68**, 3291-3294 (1992).

[6] Gang Yuan, Y. Kato, K. Murai, H. Daido, and R. Kodama *J. App. Phys.* **78** 3610 (1995).

[7] P. Celliers, F. Weber, L. B. Da Silva, T. W. Barbee, Jr., R. Cauble, A. S. Wan, and J. C. Moreno, Opt. Lett., **20**, 18 (1995).

[8] R. F. Smith, J. Dunn, J. R. Hunter, J. Nilsen, S. Hubert, S. Jacquemot, C. Remond, R. Marmoret, M. Fajardo, P. Zeitoun, L. Vanbostal, C. L.S. Lewis, M. F. Ravet and F. Delmotte, Opt. Lett., **28**, 22 (2003).

[9] A. Klisnick, O. Guilbaud, D. Ros, K. Cassou, S. Kazamias, G. Jamelot, J.-C. Lagron, D. Joyeux, D. Phalippou, Y. Lechantr, M. Edwards, P. Mistry and G. J. Tallents, J. Quant. Spect. Rad. Trans. **99**, 370-380 (2006).

[10] M. Born and E. Wolf, *Principles of Optics*, 7th ed. (Cambridge University Press, Cambridge, 1959) p504.

[11] P. Gallant, P. Forget, F. Dorchies, Z. Jiang, J. C. Kieffer, P. A. Jaanimagi, J. C. Rebuffie, C. Goulmy, J. F. Pelletier and M. Sutton, Rev Sci. Instrum., **71**, 3627-3633 (2000).

[12] M Kalal and G J Tallents, discussion (2005).

[13] P. Mistry, G J Tallents and M Kalal, Proc. SPIE **5919** (2005).

[14] G. J. Pert, J. Opt. Soc. Am. B, **11**, 8 (1994).

[15] L. W. Casperson, J. Appl. Phys. **48** 256 (1977).

[16] J. W. Goodman, "Statistical Optics" (Wiley, New York, 1985).

[17] O. Guilbaud, M. Edwards, A. Klisnick, D. Ros, G. Jamelot, D. Joyeux, D. Phalippou, H. Tang, P. Neumayer, D. Ursescu, G. Tallents, T. Kuehl, K. Cassou, K. Bouhouch, M. Kado, M Nishikino, Kota Sukegawa, M. Kishimoto, M. Ishino, K. Nagashima, H. Daido, W. Seelig, S. Borneis, E. Gaul, W. Geithner, C. Hafner and P. Wiewior, in Proceedings of SPIE Soft X-ray lasers and applications V, edited by E. Fill, S. Suckewer, vol. **5197** (SPIE, Bellingham, WA, 2003), p. 17.

[18] J.A. Plowes, G.J. Pert, S.B. Healy and D.T. Toft, Opt. Quantum Electron. **28**, 219 (1996).

[19] R H Dicke, Phys. Rev. **89**, 472 (1953).

[20] H R Griem, Phys. Rev. A**33,** 3580 (1986).

[21] F Pollock and R London, Phys. Fluids B**5**, 4495 (1993).

[22] O Guilbaud *et al,* Eur. Phys. J. D. 00154-7 (2006).

[23] L. B. Da Silva *et al.*, *Opt. Lett.* **18**, 1174 (1993).

Captions

Figure 1: The short pulse duration reduction *f* in fringe visibility as a function of optical path difference Δt (in units of pulse duration *T*), for Gaussian (—) and asymmetric sech (*A*=1 and *B*=8) (·····) shaped pulses (see equation 5).

Figure 2: (Color online) Spectral intensity variation of the x-ray laser output assuming a Gaussian gain coefficient profile of FWHM $\Delta\upsilon_G$. Intensities are shown for difference gain length products *G(0)L* (as labelled) relative to the line center.

Figure 3: (Color online) The variation in the degree of coherence with path difference for different actual gain coefficient length products *G(0)L* assuming a Gaussian gain coefficient profile of frequency FWHM $\Delta\upsilon_G$.

Figure 4: (Color online) Spectral intensity variation of the x-ray laser assuming a Lorentzian gain coefficient profile of FWHM $\Delta\upsilon_L$. Intensities are shown for different gain length products *G(0)L* (as labelled) relative to the line center.

Figure 5: (Color online) The variation in the degree of coherence with path difference for different actual gain coefficient length products *G(0)L* assuming a Lorentzian gain profile frequency FWHM $\Delta\upsilon_L$.

Figure 6: (Color online) Spectral intensity variation of the x-ray laser assuming a Voigt gain coefficient profile produced by convoluting Gaussian and Lorentzian gain coefficient profiles of equal spectral widths. The width of the resulting Voigt gain coefficient is $\Delta\upsilon_V$ (FWHM).

Figure 7: (Color online) The variation in the degree of coherence with path difference for different actual gain coefficient length products *G(0)L* assuming a Voigt gain coefficient profile produced by convoluting Gaussian and a Lorentzian gain coefficient profiles of equal spectral widths. The width of the resulting Voigt gain coefficient is $\Delta\upsilon_V$ (FWHM).

Figure 8: (Color online) The variation in the longitudinal coherence length $\Delta t\Delta\upsilon$ with actual gain coefficient length product *G(0)L* for Gaussian (——), Lorentzian (– –) and Voigt (·····) gain coefficient profiles of FWHM $\Delta\upsilon$. The sample Voigt profile is assumed to have equal spectral width contributions from Gaussian and Lorentzian components.

Figure 9: Measured visibilities (ν) from Klisnick *et al*. [9] with L = 1 cm and averaged corrected visibilities (9) as a function of optical path difference in the interferometer. The corrected visibilities are adjusted to allow for the short pulse duration of the pulse and are shown with error bars following the published range of experimental observations. Calculated variations of the degree of coherence for different gain-length $G(0)L$ products (as marked) for a Gaussian gain coefficient of bandwidth $\Delta\upsilon$ = 6.5×10^{11} Hz are also shown.

Figure 10: The variation of the full width at half maximum of the x-ray laser pulse duration with target length measured experimentally (data points) and simulated with the EHYBRID and RAYTRACE codes (solid curve). The transform limited values for $\Delta\upsilon = 6.5\times10^{11}$ Hz and 9.5×10^{11} Hz for different gain coefficients $G(0)$ are also shown (as labeled).

Figure 11a-d: (Color online) Experimental (solid line) and the convolution of the transform limit intensity variation (arb. Units) with an EHYBRID/RAYTRACE calculated temporal profile of the x-ray laser output (broken line) for target lengths of 5, 7, 10 and 15 mm (a, b, c, and d respectively). A gain profile width of $\Delta\upsilon = 9.5\times10^{11}$ Hz and gain coefficient $G(0) = 18$ cm^{-1} is assumed for the calculated temporal profiles.

Figure 12: The experimental visibility data (□) for a plasma of 30 mm length reported by Celliers *et al*. [7], the Gaussian best fit (– –) and our calculated visibility fitting for *G(0)L*=7 (——) for the experiment.

Figure 13: The raw experimental visibility data (□) for a plasma length of 1.25 cm, the Gaussian best fit (– –) and calculated visibility fit for *G(0)L*=18.00 (——) for a 6 ps CPA pumping beam and $\Delta\upsilon_G = 1.95\times10^{12}$ Hz. The visibility data and the Gaussian best fit are taken from Smith *et al*. [8].

Figure 14: As figure 13 except for a 13ps CPA pulse and $\Delta\upsilon_G = 1.67\times10^{12}$ Hz.

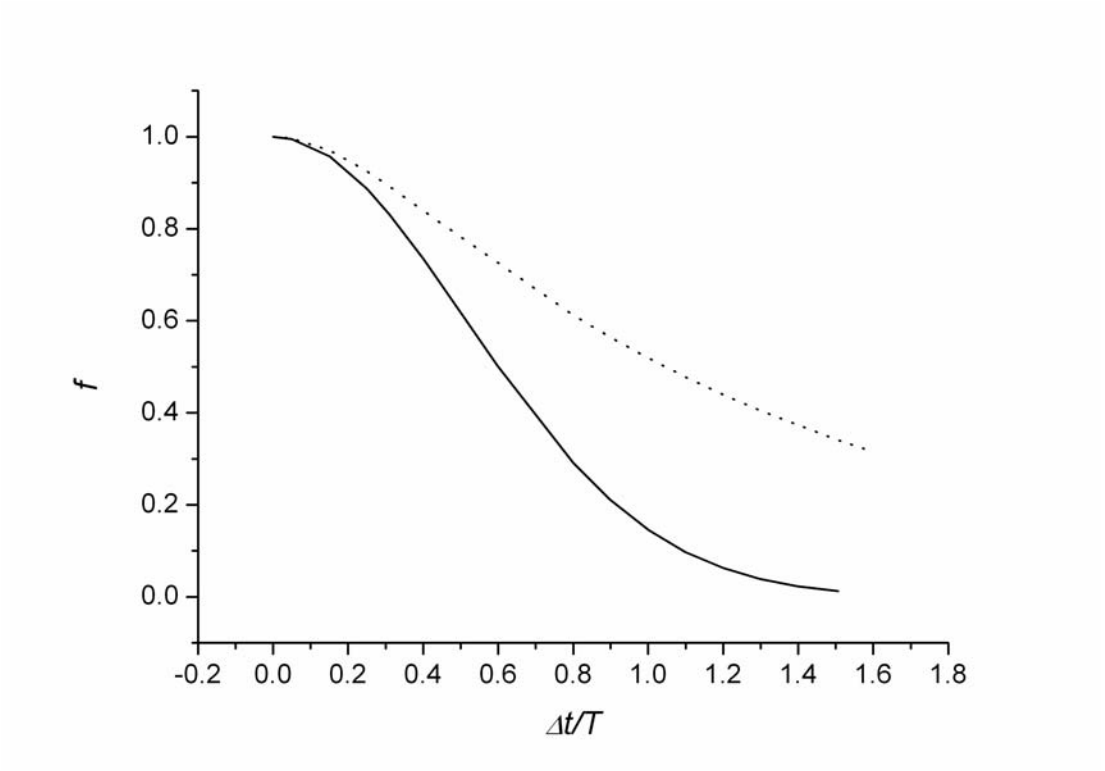

Figure 1

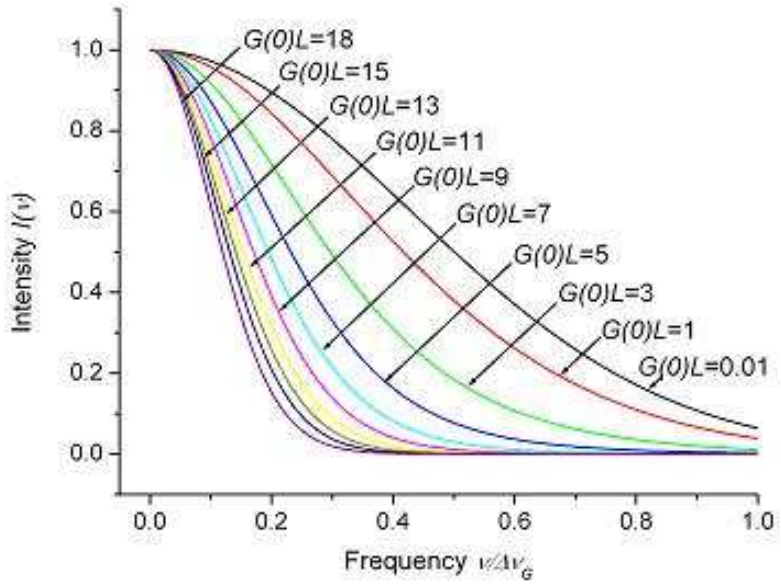

Figure 2

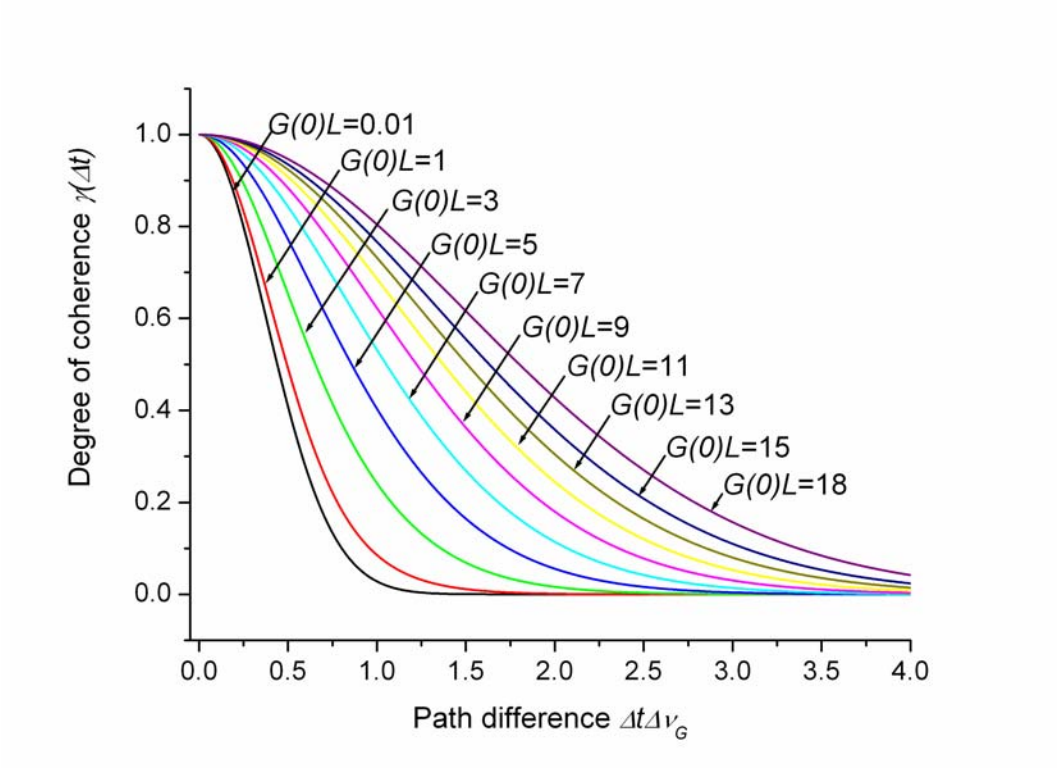

Figure 3

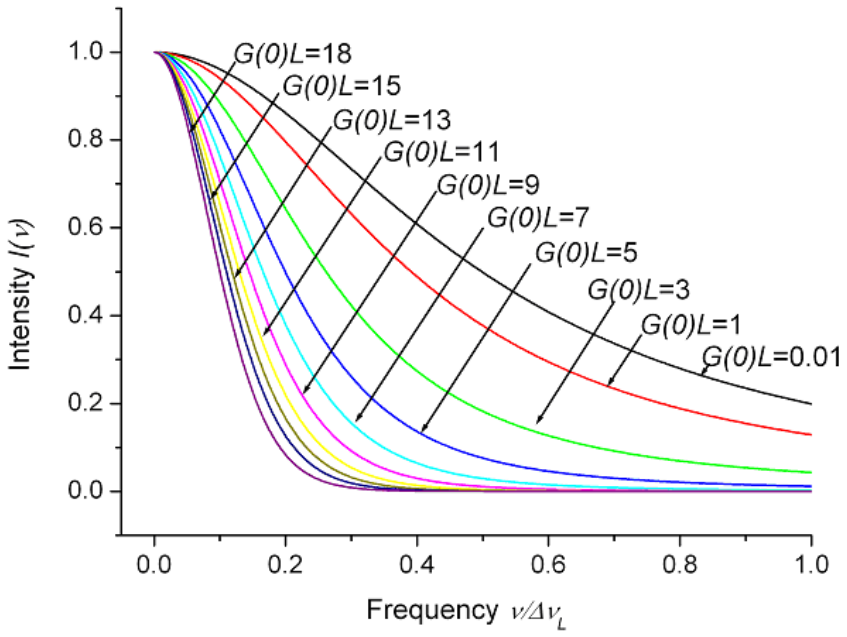

Figure 4

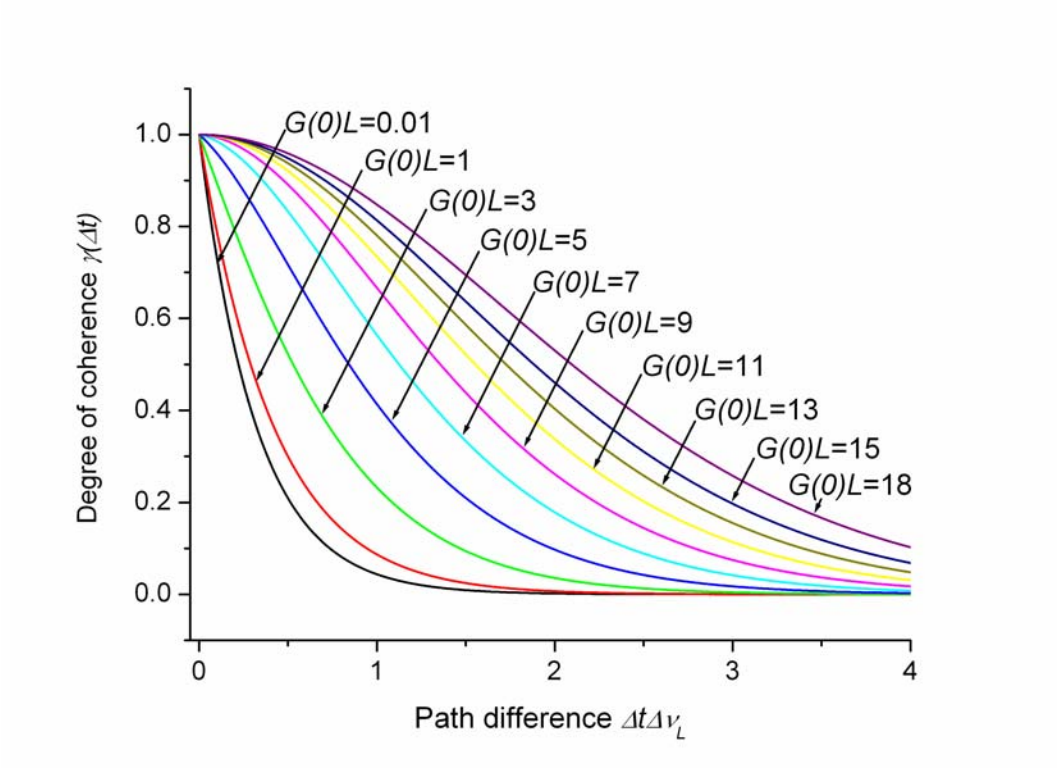

Figure 5

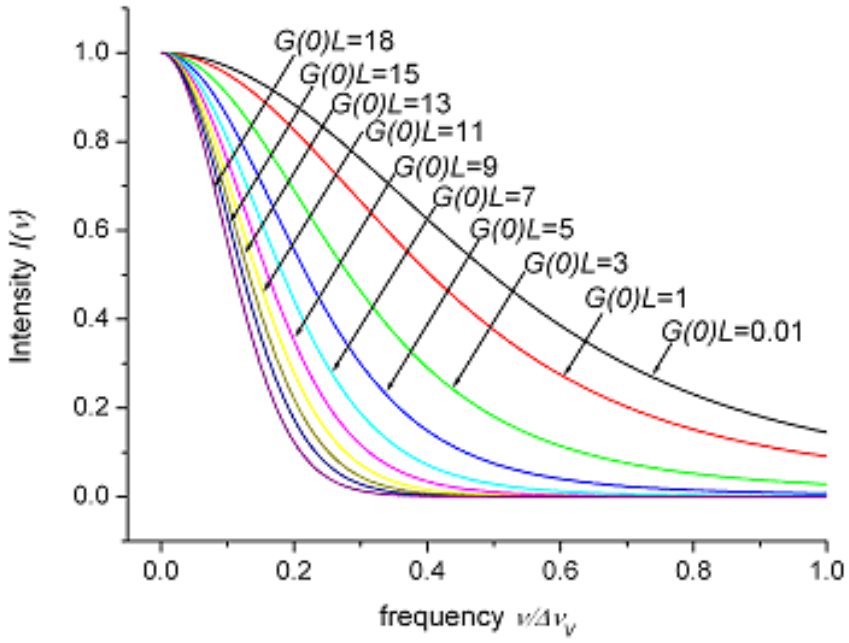

Figure 6

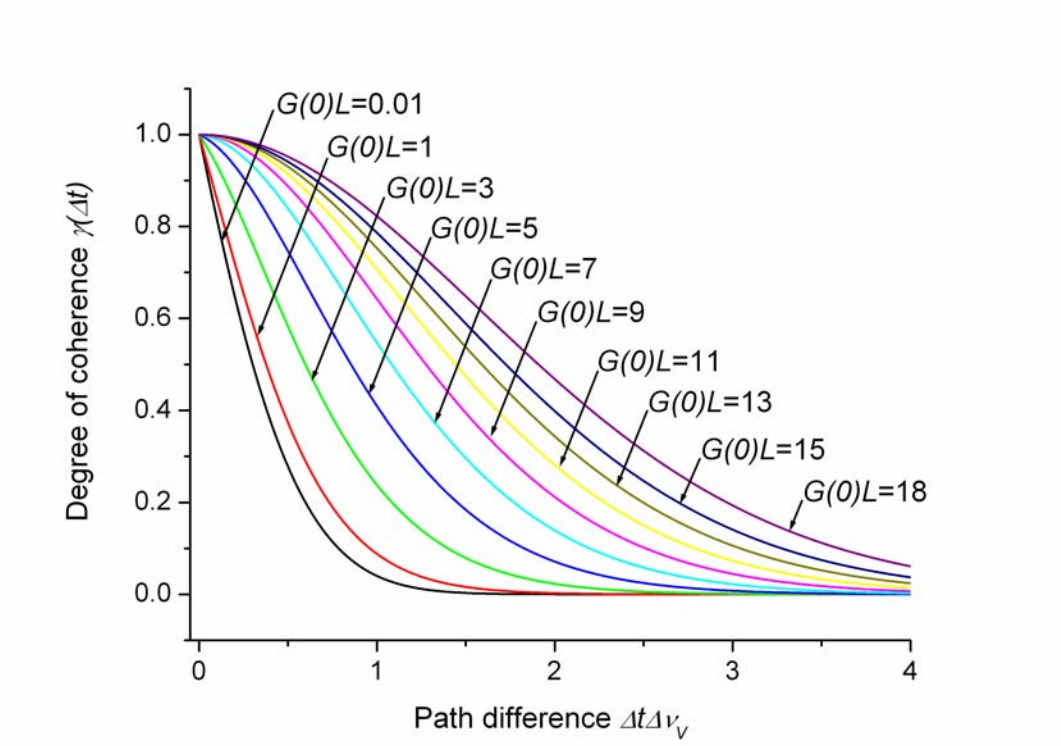

Figure 7

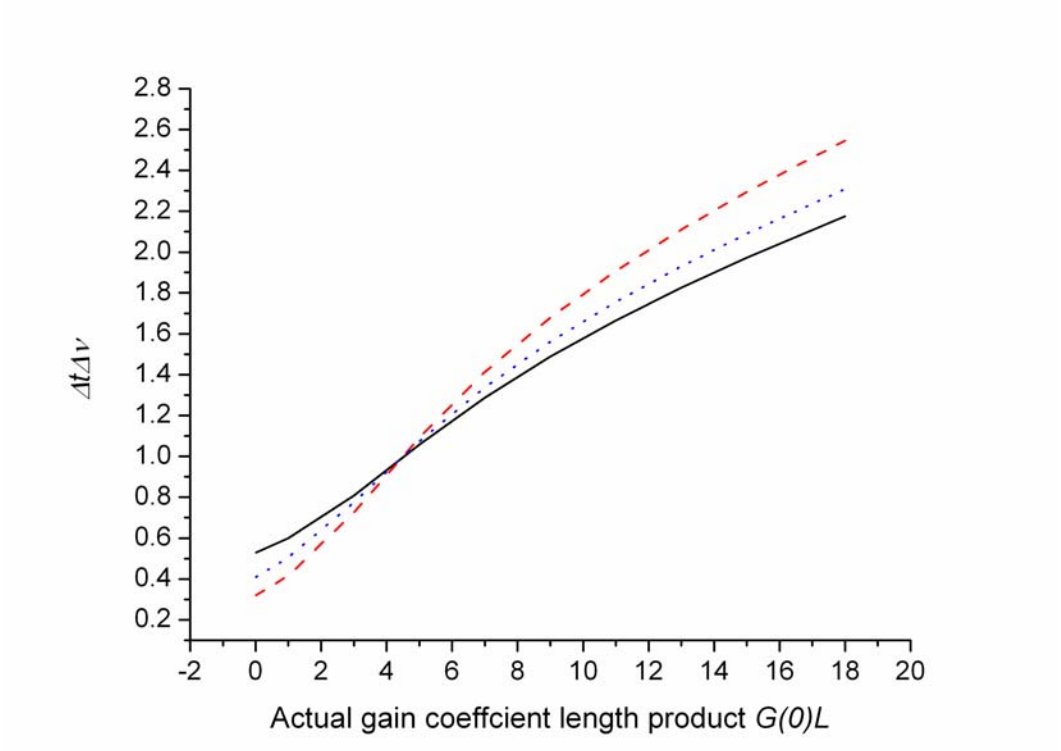

Figure 8

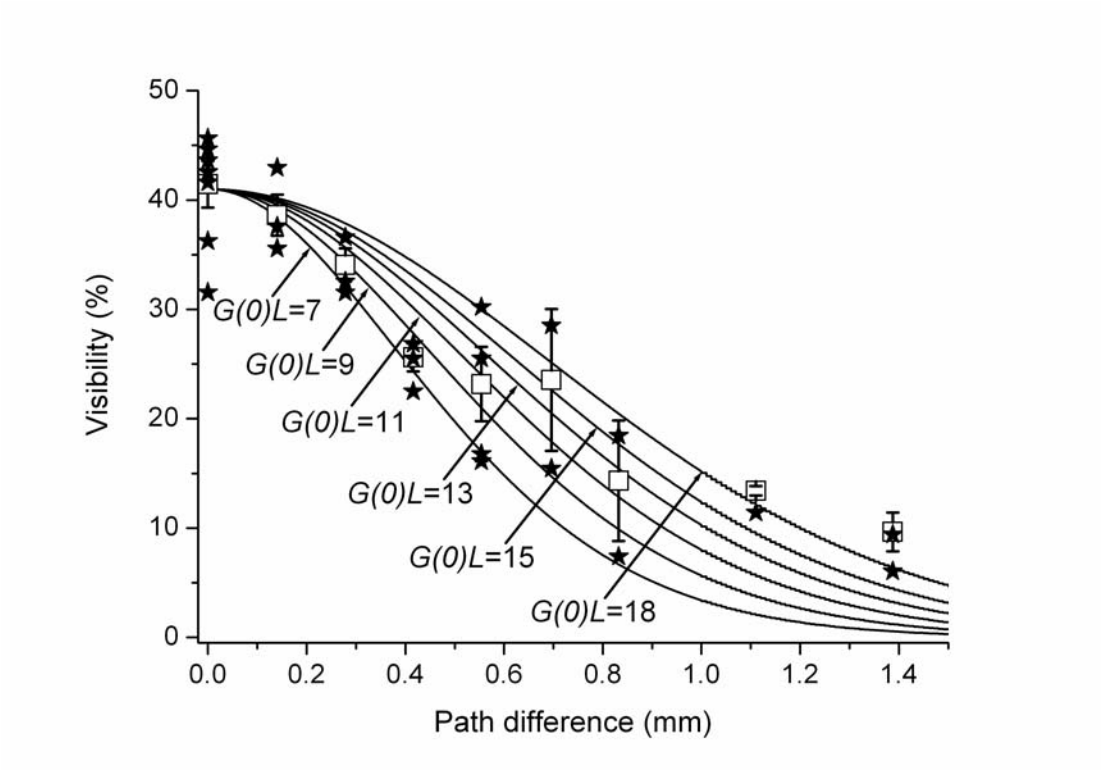

Figure 9

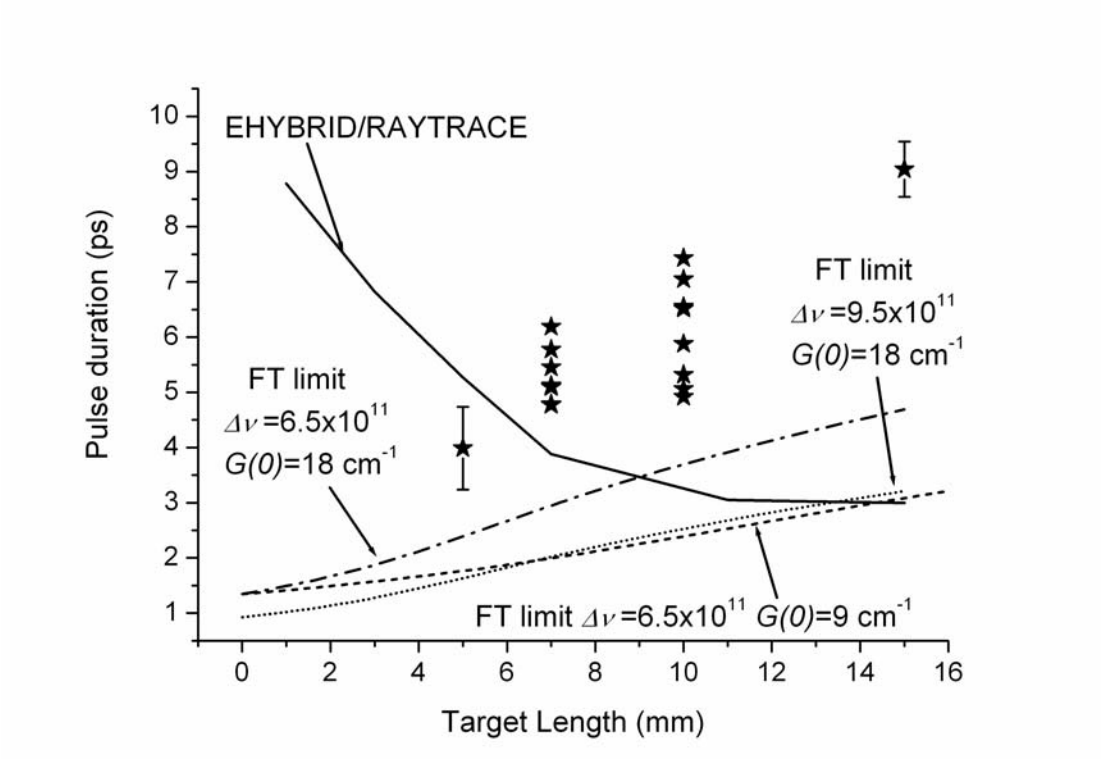

Figure 10

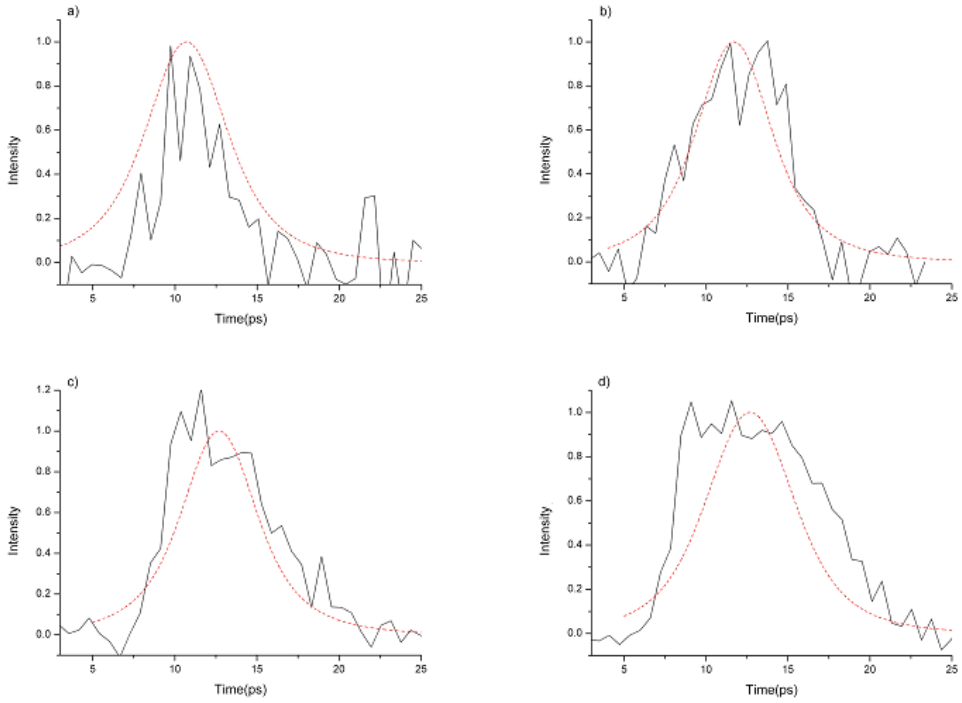

Figure 11a-d

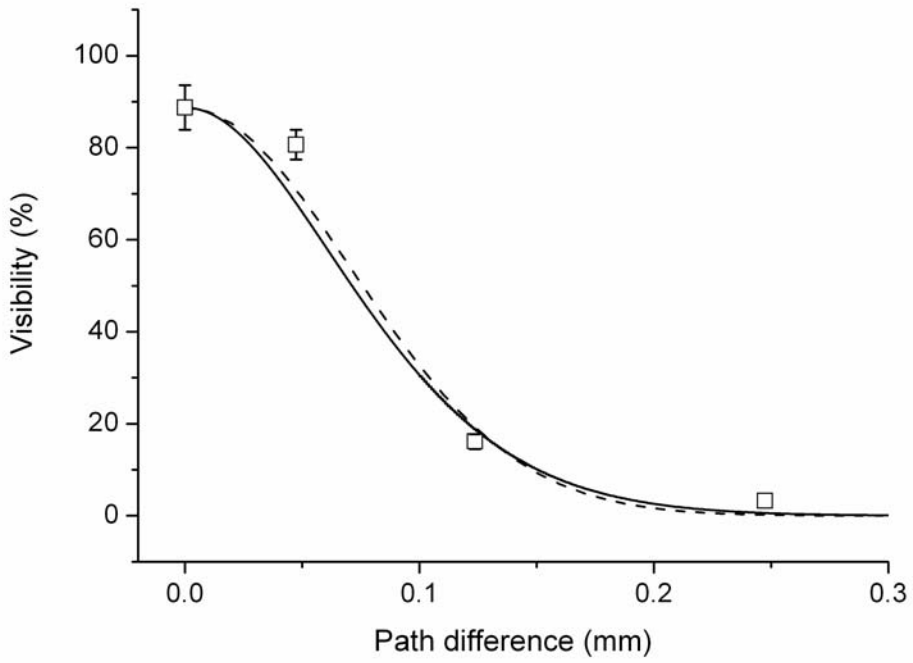

Figure 12

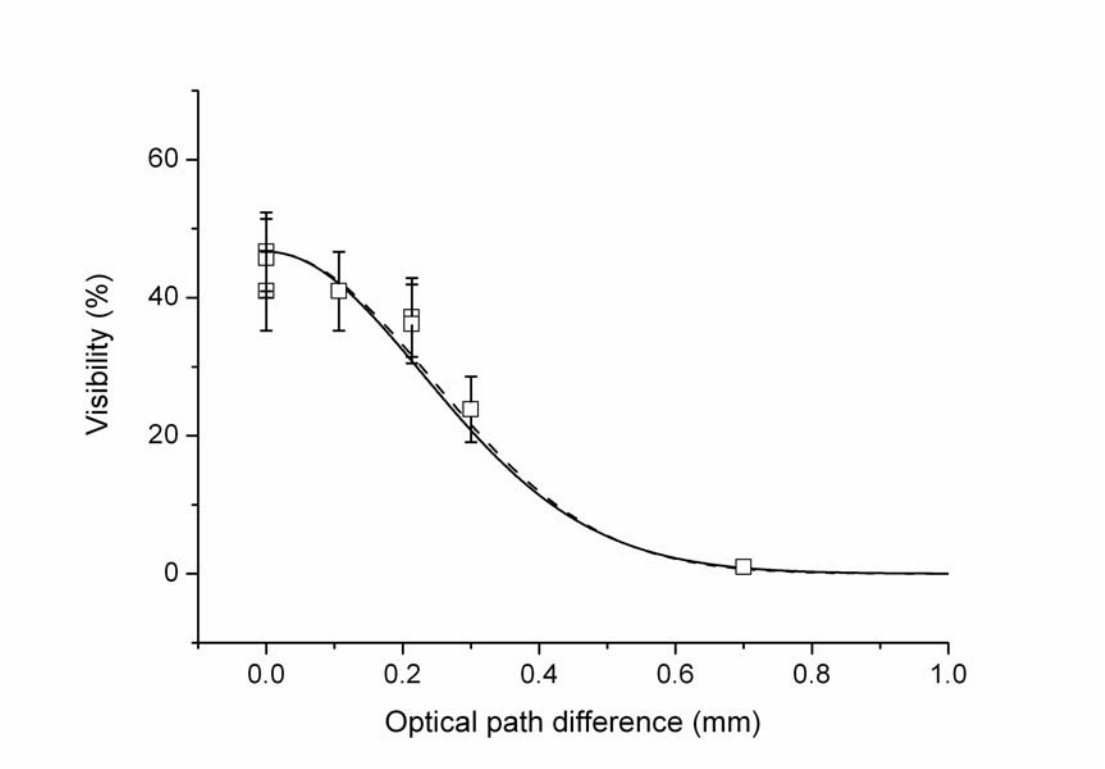

Figure 13

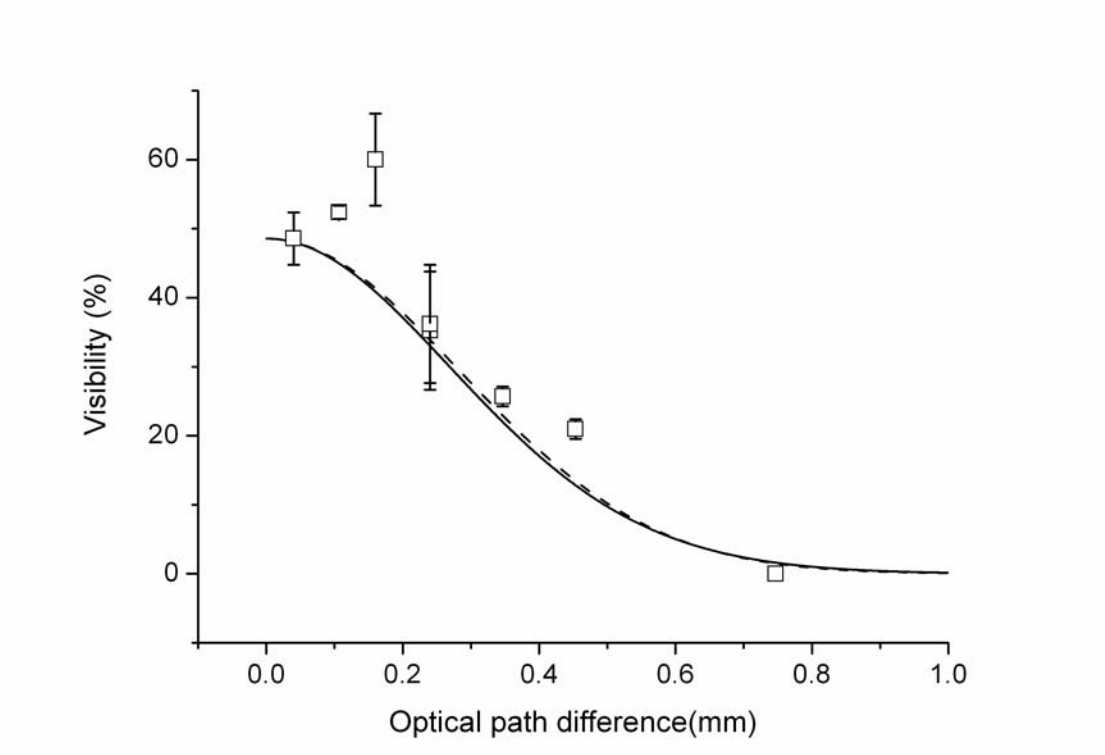

Figure 14